Feasibility check: can audio be a simple alternative to force-based feedback for needle guidance?

Alfredo Illanes[1][0000−0002−0118−0483], Axel Boese[1][0000−0002−5874−7145], Michael Friebe[1][0000−0002−8624−0800], and Christian Hansen[1,2][0000−0002−5734−7529]

[1] University of Magdeburg, Universitätsplatz 2, 39106 Magdeburg, Germany
`alfredo.illanes@ovgu.de`
[2] Research Campus STIMULATE, Sandtorstrasse 23, 39106 Magdeburg, Germany

Abstract. Accurate needle placement is highly relevant for puncture of anatomical structures. The clinician's experience and medical imaging are essential to complete these procedures safely. However, imaging may come with inaccuracies due to image artifacts. Sensor-based solutions have been proposed for acquiring additional guidance information. These sensors typically require to be embedded in the instrument tip, leading to direct tissue contact, sterilization issues, and added device complexity, risk, and cost. Recently, an audio-based technique has been proposed for "listening" to needle tip-tissue interactions by an externally placed sensor. This technique has shown promising results for different applications. But the relation between the interaction event and the generated audio excitation is still not fully understood. This work aims to study this relationship, using a force sensor as a reference, by relating events and dynamical characteristics occurring in the audio signal with those occurring in the force signal. We want to show that dynamical information that a well-known sensor as force can provide could also be extracted from a low-cost and simple sensor such as audio. In this aim, the Pearson coefficient was used for signal-to-signal correlation between extracted audio and force indicators. Also, an event-to-event correlation between audio and force was performed by computing features from the indicators. Results show high values of correlation between audio and force indicators in the range of 0.53 to 0.72. These promising results demonstrate the usability of audio sensing for tissue-tool interaction and its potential to improve telemanipulated and robotic surgery in the future.

Keywords: Audio guidance · Force feedback · Needle interventions.

1 Introduction

Percutaneous needle insertion is one of the most common minimally invasive procedures. The experience of the clinician is an important requirement for accurate placement of needles, given the reduced visual and tactile information transmitted to the clinician via the instruments. Imaging techniques such as magnetic

resonance, computed tomography, or ultrasound can support clinicians in this type of procedure, but the accuracy can still not be fully assured because of artifacts present in the images [20, 14].

Sensor-based solutions have been proposed for providing haptic feedback during the procedure [11, 10, 18, 7, 8, 1, 5, 12, 23, 19, 3]. However, most of these solutions require sophisticated sensors that sometimes need to be embedded in the instrument tip or shaft, leading to direct contact with human organs, sterilization issues, the use of non-standard and quality-reduced tools, added device complexity, risk and cost. This imposes serious design limitations, and therefore they have encountered difficulties in being adopted for regular clinical use.

Recently, an audio-based technique has been proposed in [9] for *listening* to the needle tip-tissue interaction dynamics using a sensor placed at the proximal end of the tool. The authors of this work has shown promising preliminary results for monitoring medical interventional devices such as needles [9], guide wires [15], and laparoscopic tools [4]. However, even if audio has proved to be a tool with potential for providing guidance information such as tissue-tissue passage, puncture and perforation events or palpation information, the generated audio dynamics are still not fully understood.

The aim of this work is to investigate the audio dynamics generated from needle-tissue interactions during needle insertion to have a better understanding of the generation of the audio excitation using the audio-based guidance technique. In this purpose, force is used as a reference since it has been widely employed in the literature to understand interactions between needles and tissue. The main idea is to relate events and dynamical characteristics extracted from the audio signal with those extracted from the force signal through indicators and event features computed by processing both signals. The audio signal is processed by extracting its homomorphic envelope. Indicators related to local event intensity, derivative, and curvature are computed from the force signal. The Pearson coefficient is used for signal-to-signal correlation between audio and force indicators. Then, event-to-event correlation between audio and force events is performed by computing features from the indicators.

Results show values of Pearson coefficient between audio and force indicators in the range of 0.53 to 0.72, being the highest one the correlation of audio with force curvature. Additionally, events of high correlated indicators exhibit a clear relationship that can be important for understanding audio behavior. Both analyses show that audio, acquired non invasively with a simple and low-cost sensor, can contain significant information that can be used as additional feedback to clinicians.

2   Method

Needle insertion and its interaction with soft tissue has been widely studied using force sensors, being possible to distinguish three phases of interaction [17, 2, 6]. During the first phase or pre-puncture phase, the needle tip deforms the surface in contact with the tissue producing an increase in the force. The second

phase starts with the puncture event or tissue breakage, characterized by a peak in the force, followed by a sharp decrease. The third phase corresponds to the post-puncture phase, where the force can vary due to friction, collision with interior structures, or due to the puncture of a new tissue boundary. During the first phase, when audio is acquired, no audio excitation occurs since there is no tissue breakage or structure collision. The puncture during the second phase and the collisions, friction, and new punctures during the second and third phases can produce significant and complex audio excitation dynamics. However, even if an audio response is complicated, its dynamics should be related to dynamical characteristics of the force during the second and third phases. This is what we want to explore in this work.

Our aim is to extract characteristics or *feature indicators* from the force that can be related to dynamical characteristics of the audio excitation. The first indicator that we want to explore is the local intensity of the force or detrended force, which aims to emphasize the increase of force from a local deflection (contact of needle tip with the tissue) passing through its peak (puncture event) and coming back to a steady stage. We also believe that the cumulative energy stored during the boundary displacement and the fast drop in force after the puncture also influences the audio excitation, and this is why derivative and curvature indicators are also extracted.

The idea of this work is not to explain mechanical properties and fundamentals of needle insertion in soft tissue, but to demonstrate that characteristics of audio and force, even resulting from sensors of entirely different nature, can be strongly related through a sort of transfer function between both sensor modalities. Through this relationship, we also want to show the wealth of information that an audio signal can contain concerning tip-tissue interaction dynamics.

Fig. 1 displays a block diagram with the main steps to relate audio and force characteristics. First, the audio signal and the force signal are processed in order to compute the different indicators extracted for enhancing the signal features that want to be compared: one audio indicator (IA), and four force indicators, related to the local intensity (IF_i), to the curvature (IF_c), to the derivative (IF_d), and one indicator that integrates curvature and intensity (IF_{ci}). Then, a signal-to-signal correlation is performed between audio and force indicators in order to assess similarity between features and also for optimizing the parameters of the processing algorithms. Finally, an event-to-event correlation is performed by computing features from the extracted indicators.

2.1 Experimental setup and data acquisition

For evaluating the presented approach, the dataset generated in [9] was used, where audio signals were recorded using a stethoscope connected to a microphone attached to the proximal end of a needle via a 3D printed adapter (see Fig. 2a). This dataset consists of 80 audio recordings acquired during automatic insertion of an 18G 200mm length biopsy needle (ITP, Germany) into an ex-vivo porcine tissue phantom (see Fig. 2b). The insertion was performed automatically using a testing machine (Zwicki, Zwick GmbH & Co.KG, Ulm) at an insertion velocity of
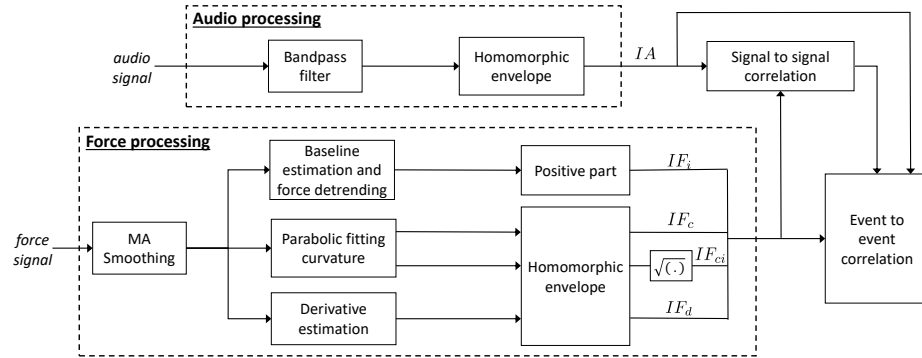
Fig. 1. General block diagram with the methodology to relate force and audio signals.

3 mm/s that also recorded the axial needle insertion force. The audio frequency sampling was 44100 Hz, and one force sample was acquired every 0.03 mm. If we assume the velocity nearly constant, the force sampling frequency can be estimated at around 100 Hz. The acquisition of force and audio was synchronized using a trigger event visible in both the force and audio signals.
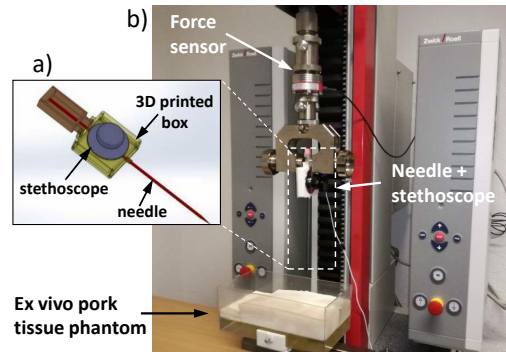

Fig. 2. Experimental setup for needle insertion in fat tissue (adapted from [9]).

2.2   Audio indicator extraction

The audio signal is first pre-processed using a 7th-order Butterworth bandpass filter $(3-6$ KHz$)$ in order to enhance the needle tip tissue interaction information, as shown in [9].

Fig. 3 displays the filtered audio signal together with the synchronized force signal during needle insertion into soft tissue, using a recording from the dataset presented in [9], which will be introduced in Section 3. It is possible to observe

from the three marked events (denoted by 1, 2 and 3) in Fig. 3(a) and (b) and the zooms in Fig. 3(c), that a main puncture event, identifiable in the force as a significant peak, exhibits a complicated succession of events in the audio signal. This set of events denotes the accumulation of energy through modulation of the signal amplitude at the time interval just after the rupture of the tissue. To represent this energy event accumulation, we compute the homomorphic envelope of the audio signal, which represents the amplitude modulation of the signal and that it is obtained using homomorphic filtering in the complex domain [21].
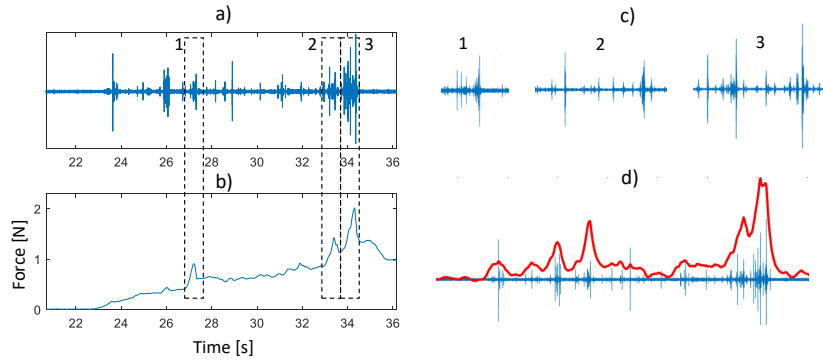
Fig. 3. (a) Bandpassed audio signal with labeled main puncture events. (b) force signal with labeled main puncture events. (c) Audio zoom over the puncture events. (d) Homomorphic envelope of the audio signal.

2.3   Force processing for indicators extraction

As explained above, four indicators are extracted from the force signal by enhancing information related to characteristics such as intensity, derivative, and curvature. The diagram of Fig. 1 shows the main steps for the computation of the force indicators. The first step that is common to all the indicators is the force signal smoothing, consisting of the application of a moving average filter in order to reduce the high-frequency ripple dynamics from the force.

The force indicator IF_i intends to extract the information concerning the local intensity of the force. In this aim, a force detrending has to be performed to attenuate the very low-frequency progression present in the force signal during needle insertion. For that, the signal baseline is first estimated using a two-stage median filter [22] that is then subtracted to the smoothed force signal. Finally, the positive part of the resulting signal is extracted.

For the computation of the force indicator related to the derivative IF_d, a derivative filter in series with a smoothing filter is first applied following [13]. To only keep the most important positive characteristics of the derivative, the homomorphic envelope is extracted.

The curvature is estimated with the algorithm proposed in [16] that enhances curvature and intensity in signals. A 2nd-degree polynomial is used to fit the force signal inside a sliding window. The 2nd-degree coefficient is related to the curvature of the signal. The force indicator IF_c is finally computed by applying a homomorphic envelope to the resulting curvature.

As explained in [16], an indicator that enhance intensity and curvature jointly can be extracted by computing the product between the constant polynomial coefficient and the 2nd-degree coefficient of the polynomial. IF_{ci} is computed as the square root of the joint indicator.

Fig. 4 shows the four extracted indicators, including also the original force signal and the baseline estimation (in red).
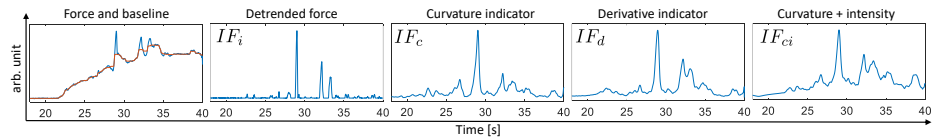
Fig. 4. Four indicators extracted from the force signal. In red color the estimated force baseline is displayed.

2.4   Force and audio information correlation methodology

Two approaches are applied for putting in relation the indicators extracted from the force with the one extracted from the audio. A signal-to-signal correlation using the Pearson coefficient is first performed. This step allows assessing the similarity between both types of indicators and also to optimize the parameters involved in the computation of the indicators. In fact, the extraction of the force and audio indicators requires to set some parameters:

- The frequency cut-off of the low-pass filter to be used in the envelope extraction for the audio and force signals, denoted as lpf_a and lpf_f, respectively.
- The length of the sliding window used for computing the polynomial fitting of the force signal, denoted as h_{win}.
- The first and second stage averaging window length of the median filter applied for the force detrending, denoted by L_1 and L_2, respectively.

Each parameter is optimized by maximizing the Pearson coefficient between the force indicator and the audio indicator.

Using the optimized parameters, we perform an event-to-event correlation analysis. Significant puncture events in the force are first detected using a standard peak detector algorithm. Then, a window W is defined around the detected peak instant in the audio signal. Finally, for each detected event, we relate the maximal value of the force indicator inside W to the energy of the audio indicator, also inside W.

3   Results

Table 1 shows the optimized results of the correlation between the four force indicators and the audio indicator. The table also shows the values of the parameters for the extraction of the indicators. In bold are marked the parameters that required optimization (lpf_a, L_1, L_2, h_{win}, and lpf_f). The span of the MA smoother used for the computation of the force indicators was set to 10 samples, equivalent to 0.1 seconds for a sampling frequency of 100 Hz. The last column of the table shows the average optimized Pearson coefficient value ($\overline{\rho}$) over the 80 recordings of the dataset. It is possible to observe that the best correlation between audio and force is obtained with the force curvature indicator. It is important to notice in the table, in the second column from the end, that the average and standard deviation values of the correlation coefficient obtained during optimization do not vary significantly when the parameters are modified.

Table 1. Average optimized Pearson coefficients for the correlation between the four force indicators and the audio indicator for the 80 needle insertion audio recordings.

| Comparison	Audio Parameters	Force Parameters					$mean \pm std$	$\overline{\rho}$
	$\mathbf{lpf_n}$	MAspan	$\mathbf{L_1}$	$\mathbf{L_2}$	$\mathbf{h_{win}}$	$\mathbf{lpf_f}$		
IA vs IF_i	4	10	100	100	n/a	n/a	0.489 ± 0.038	0.531
IA vs IF_c	1	10	n/a	n/a	7	1	0.611 ± 0.038	0.717
IA vs IF_d	1	10	n/a	n/a	n/a	1	0.511 ± 0.061	0.664
IA vs IF_{ci}	1	10	n/a	n/a	13	1	0.578 ± 0.050	0.672

Fig. 5 displays a further analysis concerning the obtained correlation Pearson coefficients. In Fig. 5(a), the histograms of the Pearson coefficients between the four force indicators and the audio indicator are displayed. It is possible to verify that the correlation values range in general between 0.3 and 0.9, but that for curvature and the joint curvature and intensity indicators, 50% of the recording has a correlation value over 0.6, which is high considering the completely different nature between audio and force sensors. Fig. 5(b), which shows the accumulative histogram of the Pearson coefficient, confirms the analysis made previously. It is possible to observe that the best correlation between audio and force is obtained with the curvature indicator IF_c, followed by the joint curvature and intensity indicator IF_{ci}. The derivative of the force IF_d also provides high values of correlation, while the local intensity indicator IF_i is the weakest indicator influencing the audio.

Fig. 6 shows examples of high correlations between each force indicator and the audio indicator for different recordings belonging to the dataset. It is possible to see how the main dynamics extracted from the audio indicator can follow the dynamics obtained from the force indicator, i.e., many of the information involve in force it is somehow visible in the audio indicator signal.

Fig. 7 shows the results of the event-to-event correlation of the two best correlations obtained in the signal-to-signal analysis: curvature IF_c indicator
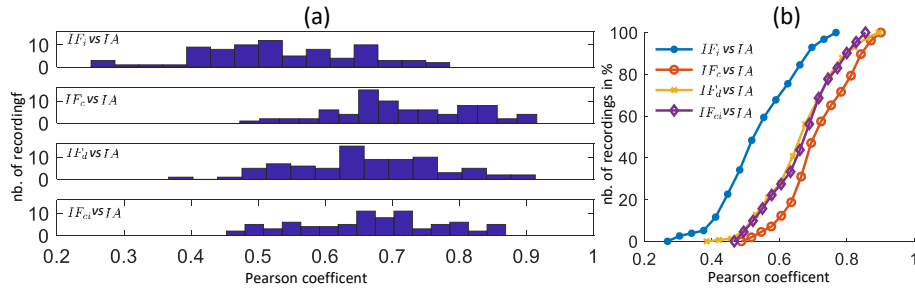
Fig. 5. Standard and cumulative histograms of the Pearson coefficients of the four force indicators with audio, for the 80 recordings.
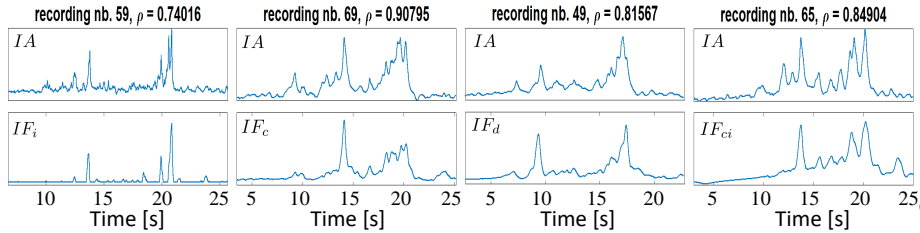

Fig. 6. Examples of force and audio indicators where high correlation were obtained.

versus the audio indicator IA and the joint curvature and intensity indicator IF_{ci} and IA. We explore two scenarios, the first one (Fig. 7(a) and (b)) by taking into account a large number of puncture events and the second one (Fig. 7(c) and (d)) by taking into account only the most important puncture events occurring during the needle insertion process. This is done by only modifying a simple threshold in the peak detector; higher is the threshold more events will be taken into account. For both force indicators, a clear event correlation can be observed using both types of event thresholding. When a large number of events are taken into account, we can see that in the range of force events presenting low intensities, it is not exactly clear that a high-intensity event will produce a high audio excitation. However, when the number of events is reduced, it is possible to observe an evident linear correlation between force and audio events, and this is even more evident with IF_{ci} in Fig. 7(c).

4   Conclusion

In this work, we explored the audio dynamics generated from the tip/tissue interaction during needle insertion into soft tissue using a recently proposed audio guidance technique. The main idea was to observe the effect of different characteristics of force measurement on the audio excitation. The results of this work do not intend to replace a force sensor but show that information resulting from sensors of entirely different natures, such as audio and force, can be strongly
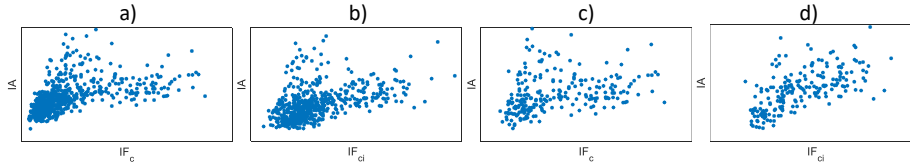
Fig. 7. Event-to-event correlation for (a) IF_c vs. IA with a low intensity-event threshold, (b) IF_{ci} vs. IA with a low intensity-event threshold, (c) IF_c vs. IA with a high intensity-event threshold, and (d) IF_{ci} vs. IA with a high intensity-event threshold.

related during needle insertion, suggesting that audio can contain valuable information for monitoring tip/tissue interaction dynamics.

The operation of such a solution in a real clinical scenario (noisy environment, variability between users) should be further tested and validated. However, preliminary results obtained in this work and [9] indicate that a tissue/tissue passage audio event can be viewed as an abrupt change detection problem regardless of the user and the insertion velocity (a signal dynamical change is produced at the border of two tissues). Additionally, a puncture results in a high energy audio excitation that may simplify the processing of the signal in noisy environments.

The next steps of this work involve the exploration of non-linear dynamical relationships between force and audio using not only time-domain energy-based features but also time-variant audio signatures using frequency, scale, or modal based features.

References

1. Abayazid, M., Kemp, M., Misra, S.: 3d flexible needle steering in soft-tissue phantoms using fiber bragg grating sensors. In: 2013 IEEE International Conference on Robotics and Automation. pp. 5843–5849. IEEE (2013)
2. Abolhassani, N., Patel, R., Moallem, M.: Needle insertion into soft tissue: A survey. Medical engineering & physics **29**(4), 413–431 (2007)
3. Chadda, R., Wismath, S., Hessinger, M., Schäfer, N., Schlaefer, A., Kupnik, M.: Needle tip force sensor for medical applications. In: 2019 IEEE SENSORS. pp. 1–4. IEEE (2019)
4. Chen, C., Sühn, T., Kalmar, M., Maldonado, I., Wex, C., Croner, R., Boese, A., Friebe, M., Illanes, A.: Texture differentiation using audio signal analysis with robotic interventional instruments. Computers in biology and medicine **112**, 103370 (2019)
5. Elayaperumal, S., Bae, J.H., Daniel, B.L., Cutkosky, M.R.: Detection of membrane puncture with haptic feedback using a tip-force sensing needle. In: 2014 IEEE/RSJ International Conference on Intelligent Robots and Systems. pp. 3975–3981. IEEE (2014)
6. van Gerwen, D.J., Dankelman, J., van den Dobbelsteen, J.J.: Needle–tissue interaction forces–a survey of experimental data. Medical engineering & physics **34**(6), 665–680 (2012)

7. Henken, K., Van Gerwen, D., Dankelman, J., Van Den Dobbelsteen, J.: Accuracy of needle position measurements using fiber bragg gratings. Minimally Invasive Therapy & Allied Technologies **21**(6), 408–414 (2012)
8. Ho, S.C.M., Razavi, M., Nazeri, A., Song, G.: Fbg sensor for contact level monitoring and prediction of perforation in cardiac ablation. Sensors **12**(1), 1002–1013 (2012)
9. Illanes, A., Boese, A., Maldonado, I., Pashazadeh, A., Schaufler, A., Navab, N., Friebe, M.: Novel clinical device tracking and tissue event characterization using proximally placed audio signal acquisition and processing. Scientific reports **8**(1), 1–11 (2018)
10. Iordachita, I., Sun, Z., Balicki, M., Kang, J.U., Phee, S.J., Handa, J., Gehlbach, P., Taylor, R.: A sub-millimetric, 0.25 mn resolution fully integrated fiber-optic force-sensing tool for retinal microsurgery. International journal of computer assisted radiology and surgery **4**(4), 383–390 (2009)
11. Kalvøy, H., Frich, L., Grimnes, S., Martinsen, Ø.G., Hol, P.K., Stubhaug, A.: Impedance-based tissue discrimination for needle guidance. Physiological measurement **30**(2), 129 (2009)
12. Kumar, S., Shrikanth, V., Amrutur, B., Asokan, S., Bobji, M.S.: Detecting stages of needle penetration into tissues through force estimation at needle tip using fiber bragg grating sensors. Journal of biomedical optics **21**(12), 127009 (2016)
13. Laguna, P., Thakor, N.V., Caminal, P., Jane, R., Yoon, H.R., de Luna, A.B., Marti, V., Guindo, J.: New algorithm for qt interval analysis in 24-hour holter ecg: performance and applications. Medical and Biological Engineering and Computing **28**(1), 67–73 (1990)
14. Lal, H., Neyaz, Z., Nath, A., Borah, S.: Ct-guided percutaneous biopsy of intrathoracic lesions. Korean journal of radiology **13**(2), 210–226 (2012)
15. Mahmoodian, N., Schaufler, A., Pashazadeh, A., Boese, A., Friebe, M., Illanes, A.: Proximal detection of guide wire perforation using feature extraction from bispectral audio signal analysis combined with machine learning. Computers in biology and medicine **107**, 10–17 (2019)
16. Manriquez, A.I., Zhang, Q.: An algorithm for qrs onset and offset detection in single lead electrocardiogram records. In: 2007 29th Annual International Conference of the IEEE Engineering in Medicine and Biology Society. pp. 541–544. IEEE (2007)
17. Okamura, A.M., Simone, C., O'leary, M.D.: Force modeling for needle insertion into soft tissue. IEEE transactions on biomedical engineering **51**(10), 1707–1716 (2004)
18. Park, Y.L., Elayaperumal, S., Daniel, B., Ryu, S.C., Shin, M., Savall, J., Black, R.J., Moslehi, B., Cutkosky, M.R.: Real-time estimation of 3-d needle shape and deflection for mri-guided interventions. IEEE/ASME Transactions On Mechatronics **15**(6), 906–915 (2010)
19. Ravali, G., Manivannan, M.: Haptic feedback in needle insertion modeling and simulation. IEEE reviews in biomedical engineering **10**, 63–77 (2017)
20. Reusz, G., Sarkany, P., Gal, J., Csomos, A.: Needle-related ultrasound artifacts and their importance in anaesthetic practice. British journal of anaesthesia **112**(5), 794–802 (2014)
21. Rezek, I., Roberts, S.J.: Envelope extraction via complex homomorphic filtering. Technical Report TR-98-9 Technical report (1998)
22. Sameni, R., Shamsollahi, M.B., Jutten, C.: Model-based bayesian filtering of cardiac contaminants from biomedical recordings. Physiological Measurement **29**(5), 595 (2008)

23. Xu, R., Yurkewich, A., Patel, R.V.: Curvature, torsion, and force sensing in continuum robots using helically wrapped fbg sensors. IEEE Robotics and Automation Letters **1**(2), 1052–1059 (2016)